

**FULL PAPER**

# Design, synthesis, and biological evaluation of new urolithin amides as multitarget agents against Alzheimer's disease

Karar T. Shukur<sup>1</sup> | Tugba Ercetin<sup>1</sup> | Chiara Luise<sup>2</sup> | Wolfgang Sippl<sup>2</sup> |  
 Okan Sirkecioglu<sup>3</sup> | Mert Ulgen<sup>4</sup> | Goknil P. Coskun<sup>4</sup> | Mine Yarim<sup>5</sup> |  
 Mustafa Gazi<sup>6</sup> | Hayrettin O. Gulcan<sup>1</sup> 

<sup>1</sup>Department of Pharmaceutical Chemistry, Faculty of Pharmacy, Eastern Mediterranean University, Famagusta, TR North Cyprus, Turkey

<sup>2</sup>Institute of Pharmacy, Martin Luther University of Halle-Wittenberg, Halle (Saale), Germany

<sup>3</sup>Department of Chemistry, Istanbul Technical University, Istanbul, Turkey

<sup>4</sup>Department of Pharmaceutical Chemistry, Faculty of Pharmacy, Acibadem University, Istanbul, Turkey

<sup>5</sup>Department of Pharmaceutical Chemistry, Faculty of Pharmacy, Yeditepe University, Istanbul, Turkey

<sup>6</sup>Faculty of Arts and Science, Eastern Mediterranean University, Famagusta, TR North Cyprus, Turkey

**Correspondence**

Hayrettin O. Gulcan, Department of Pharmaceutical Chemistry, Faculty of Pharmacy, Eastern Mediterranean University, via Mersin 10, Famagusta 99628, TR North Cyprus, Turkey.  
 Email: ozan.gulcan@emu.edu.tr

**Abstract**

A series of urolithin amide (i.e., **URO-4-URO-10** and **THU-4-THU-10**) derivatives was designed and synthesized, and their chemical structures were confirmed with spectroscopic techniques and elemental analysis. The title compounds and synthesis intermediates (**THU-1-THU-10** and **URO-1-URO-10**) were evaluated for their potential to inhibit acetylcholinesterase (AChE), butyrylcholinesterase (BuChE), and monoamine oxidase B (MAO-B). Compounds **THU-4** and **THU-8** were found to be the most potent inhibitors for the cholinesterases and MAO-B, respectively. The docking studies were also employed to evaluate the binding modes of the most active compounds with AChE, BuChE, and MAO-B. Furthermore, the moderate-to-strong activities of the compounds were also displayed in amyloid-beta inhibition and antioxidant assay systems. The results pointed out that the urolithin scaffold can be employed in drug design studies for the development of multitarget ligands acting on various cascades shown to be important within the pathophysiology of Alzheimer's disease.

**KEYWORDS**

Alzheimer's disease, amyloid beta, antioxidant, cholinesterase, MAO-B, urolithins

## 1 | INTRODUCTION

Alzheimer's disease (AD) is a progressive neurodegenerative disease, currently affecting millions of people worldwide. It ranks sixth among the disease states leading to death.<sup>[1,2]</sup> Its progressive character (i.e., as defined as mild, moderate, and severe stages, respectively) worsens the cognitive abilities with time, which results in the requirement for

extensive patient care.<sup>[3]</sup> To slow down the progression of cognitive disabilities, the current treatment employs cholinesterase inhibitors (i.e., rivastigmine, donepezil, and galantamine) concomitant to memantine, a partial antagonist of the *N*-methyl-D-aspartate receptor.<sup>[4,5]</sup>

Throughout the development of AD, neuronal loss is certain. From this perspective, there is a deficiency in the amounts of many neurotransmitters in the central nervous system (CNS).<sup>[6,7]</sup> Previous

studies especially stated the critical role of some muscarinic and nicotinic receptors having physiological functions through the endogenous agonist action of acetylcholine on these receptors, and this is significant in preserving the routine cognitive abilities.<sup>[8]</sup> The cholinesterase inhibitors used currently therefore increase the available amount of acetylcholine in CNS, which, in turn, delays the downtrend in cognitive functions.<sup>[4,9]</sup> Memantine, on the contrary, decreases calcium ion intake through extrasynaptic receptors, which is assumed to prevent excitotoxicity.<sup>[10]</sup>

It is certain that the current drugs used for the treatment of AD are limited and they lack the certain mechanism of actions that might create alternative treatment strategies. Indeed, there is more scientific focus on the last two decades for the design of novel molecules that may act on more than one mechanism, shown to be involved in the pathophysiology of AD. This approach is also referred to as multitarget-directed ligand (MTDL) design employment.<sup>[4,11,12]</sup>

AD is a very complex disease involving multifactorial pathophysiological cascades (e.g., oxidative stress, aggregation of insoluble neurotoxic amyloid beta [A $\beta$ ], and hyperphosphorylated tau protein plaques and fibers, mitochondrial dysfunction, neurodegeneration-related neuronal loss).<sup>[13,14]</sup> Therefore, MTDL-based drug design in AD research studies generally includes the design of molecules possessing cholinesterase inhibitor potential together with a neuroprotective effect through another mechanism.

Our research group has long been interested in the design of urolithin-based molecules acting on validated and nonvalidated targets of AD.<sup>[15,16]</sup> Urolithins are hydroxylated benzo[c]chromen-6-one derivatives, formed through the gastric microflora-catalyzed biotransformation reactions upon exposure to ellagitannin-rich diet,

including but not limited to berries, nuts, and pomegranate, particularly.<sup>[17]</sup> In our previous studies, we have shown that urolithins themselves can act as weak-to-moderate enzyme (i.e., cholinesterase, monoamine oxidase B [MAO-B], and cyclooxygenase) inhibitors and antioxidants.<sup>[18]</sup> This also makes urolithins important scaffolds to be utilized in drug design studies for the treatment of AD.

One of the current MTDL design studies for AD therapy involves the dual inhibition of cholinesterase and MAO-B enzymes. This approach employs the critical functions of MAO-B throughout the development of AD.<sup>[19,20]</sup> Indeed, the expression of this enzyme in the CNS is responsible for the metabolism of dopamine, and this cascade generates electrophiles (e.g., dopamine aldehyde derivatives and semiquinone metabolites) and hydrogen peroxide (i.e., a source of reactive oxygen radicals). More important, the recent studies indicated the increased expression of MAO-B within the progressive stages of AD.<sup>[21,22]</sup> Therefore, this approach employs cholinesterase inhibition to slow down the development of cognitive disabilities and provides a neuroprotective effect through MAO-B inhibition.<sup>[22,23]</sup>

On the basis of these facts, within this study, we have designed a series of urolithin-based compounds. Mainly, various amines were aimed to be connected to urolithin and tetrahydro-urolithin moieties (i.e., 7,8,9,10-tetrahydrobenzo[c]chromen-6-one derivatives as unnatural synthetic compounds) via an amide bridge. Considering the MAO-B inhibitory potential of benzo[c]chromene ring as a coumarin analog and the pharmacophore (i.e., urolithin-spacer-amine function) developed in our previous studies for cholinesterase inhibition, the title dual cholinesterase and MAO-B inhibitors were designed (Figure 1). Besides screening the enzyme (i.e., cholinesterases and MAO-B) inhibitory potential of the title molecules, the activities of

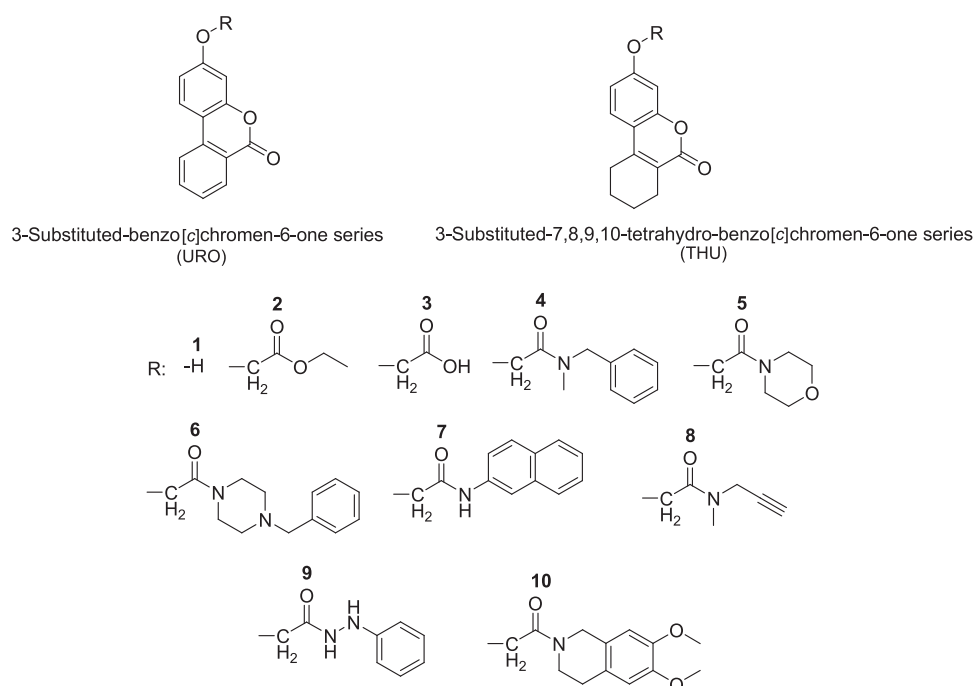


**FIGURE 1** The title molecules with synthesis intermediates. Compounds URO-1 to URO-3 and THU-1 to THU-3 are synthesis intermediates

the compounds in A $\beta$  aggregation and antioxidant assays were also aimed to be analyzed. Finally, docking studies were also employed to identify the possible receptor interactions for the most active compounds.

## 2 | RESULTS AND DISCUSSION

### 2.1 | Chemistry

The synthesis of the title molecules is shown in Scheme 1. Resorcinol was employed to obtain both **URO-1** and **THU-1** through, respectively, treating it with 2-iodobenzoic acid in basic aqueous under reflux, and ethyl 2-oxocyclohexanecarboxylate in the presence of a Lewis acid under neat conditions, according to the previously published procedures.<sup>[18,24]</sup> These two compounds were used as starting materials for the synthesis of the title URO and THU series (i.e., 6*H*-benzo[*c*]chromen-6-one and 7,8,9,10-tetrahydro-benzo[*c*]chromen-6-one derivatives, respectively). Williamson ether synthesis conditions were employed to convert **URO-1** and **THU-1**, respectively, to their ester analogs (i.e., **URO-2** and **THU-2**). Ester hydrolysis under basic conditions generated the carboxylic acid intermediates **URO-3** and **THU-3**.

To obtain the title molecules, two consecutive steps were achieved in situ employing the Schotten-Baumann technique, as previously reported.<sup>[25,26]</sup> Accordingly, thionyl chloride was used to convert carboxylic

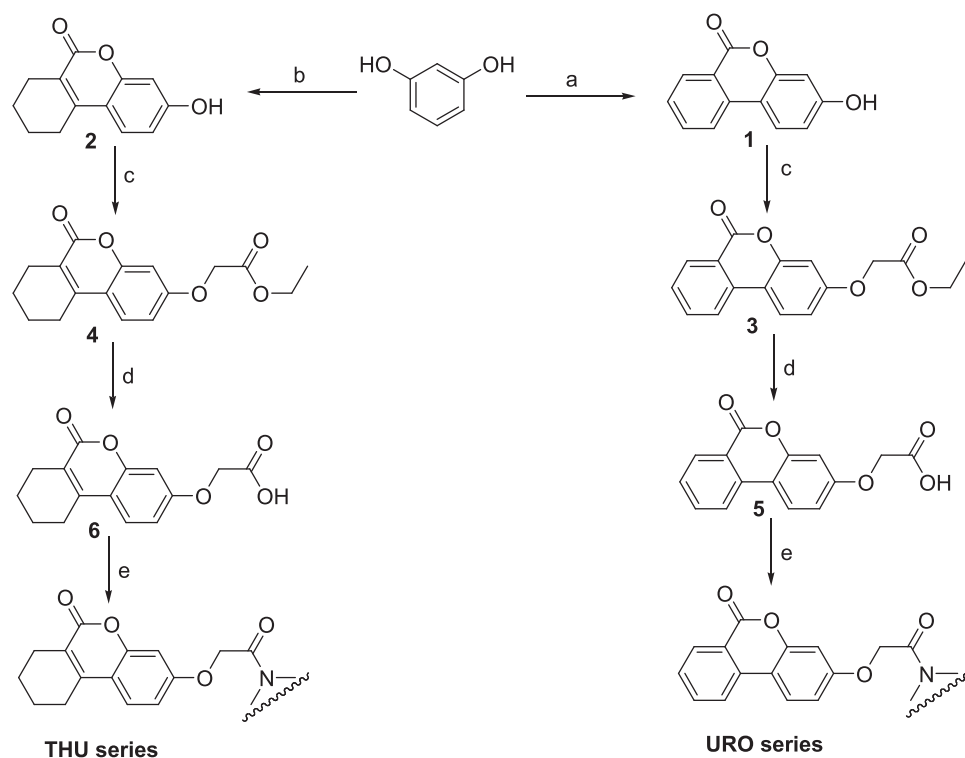
acid intermediates to their corresponding acyl chlorides. The final step synthesis of the title molecules was achieved through the in situ reaction of these unpurified acyl chloride intermediates with appropriate amines.

The structures of the synthesis intermediates and the final compounds were confirmed by spectroscopic techniques. The infrared (IR) spectra obtained displayed the carbonyl stretching shifts for the intermediates and the final compounds. <sup>1</sup>H and <sup>13</sup>C nuclear magnetic resonance (NMR) spectra concomitant to mass and elemental analysis were also evaluated for the proof of structures. Although the intermediate synthesis steps were accomplished in good yields, the final step yields were found to be moderate within the range of 50–70%.

### 2.2 | Enzyme inhibition

The potential of the compounds to inhibit cholinesterases (acetylcholinesterase [AChE] and butyrylcholinesterase [BuChE]) and MAO-B was assessed through in vitro experiments, and the results obtained are shown in Table 1.

First, the final urolithin amides (i.e., **URO-4-10** and **THU-4-10**) were found to possess an inhibitory activity toward cholinesterases within the 1–35  $\mu$ M IC<sub>50</sub> range. In general, it was observed that the final compounds of the THU series were found more active in comparison to the activities of the corresponding URO compounds. In addition, almost all the test compounds displayed slight selectivity



**SCHEME 1** The synthetic protocol followed. Reagents and conditions: (a) 2-Iodobenzoic acid, NaOH, CuSO<sub>4</sub>, H<sub>2</sub>O, reflux, 40 min; (b) ethyl 2-oxocyclohexanecarboxylate, ZrCl<sub>4</sub>, 70°C, 1 h; (c) ethyl 2-chloroacetate, NaH, dimethylformamide, rt, 1 h; (d) KOH, MeOH, reflux, 2 h; (e) two steps in situ: at first, thionyl chloride, dichloromethane (DCM), 3 h reflux, then the appropriate amine, 30 min, 0°C

**TABLE 1** The potential of the title molecules to inhibit cholinesterases and MAO-B

Title molecules	IC <sub>50</sub> (μM)		
	AChE	BuChE	MAO-B
URO-1	>50	>50	42.4 ± 1.6
URO-2	35.9 ± 1.1	>50	41.8 ± 0.1
URO-3	>50	>50	37.0 ± 0.9
URO-4	2.5 ± 0.2	4.4 ± 0.1	27.4 ± 1.0
URO-5	13.8 ± 0.7	17.0 ± 0.4	34.8 ± 0.9
URO-6	2.0 ± 0.1	4.1 ± 0.3	30.1 ± 0.2
URO-7	8.3 ± 0.1	13.6 ± 1.1	28.6 ± 0.5
URO-8	11.9 ± 0.6	14.6 ± 0.3	15.0 ± 0.4
URO-9	7.2 ± 0.4	9.9 ± 0.7	18.3 ± 0.7
URO-10	7.9 ± 0.5	9.3 ± 0.1	27.5 ± 0.2
THU-1	29.6 ± 0.4	31.1 ± 0.6	35.3 ± 1.1
THU-2	28.2 ± 0.6	35.8 ± 0.5	37.5 ± 0.4
THU-3	30.1 ± 0.2	33.7 ± 0.4	36.1 ± 0.8
THU-4	1.3 ± 0.1	1.9 ± 0.2	22.5 ± 0.4
THU-5	10.5 ± 0.3	14.3 ± 0.7	27.6 ± 0.1
THU-6	1.7 ± 0.2	3.0 ± 0.2	24.3 ± 1.1
THU-7	7.0 ± 0.3	12.1 ± 0.1	23.5 ± 0.3
THU-8	6.5 ± 0.3	8.9 ± 0.3	12.1 ± 0.8
THU-9	6.0 ± 0.1	10.4 ± 0.2	17.9 ± 0.4
THU-10	8.3 ± 0.4	10.5 ± 0.4	22.8 ± 1.2
Reference molecules			
Donepezil	0.3 ± 0.01	9.0 ± 0.1	NT
Rivastigmine	28.1 ± 0.2	11.4 ± 0.1	NT
Pargyline	NT	NT	2.2 ± 0.3

Abbreviations: AChE, acetylcholinesterase; BuChE, butyrylcholinesterase; MAO-B, monoamine oxidase B; NT, not tested.

toward AChE. Among the compounds tested, **THU-4** was found to be the most potent inhibitor for both AChE and BuChE, followed by **THU-6**, **URO-4**, and **URO-6** compounds. The common point within the structural organization of these derivatives is the presence of a methylene group bridging the nitrogen atom and the phenyl ring. On the contrary, none of the final amide compounds were found superior to the activity of donepezil against AChE. However, the AChE and BuChE inhibitory potentials of the majority of the final compounds in both URO and THU series were found superior or comparable to the activity of rivastigmine on both enzymes. Similarly, many title compounds also displayed higher activity in terms of inhibition of BuChE in comparison to the activity of donepezil under the experimental conditions utilized.

The synthesis intermediates of both URO and THU series (i.e., **URO-1-3** and **THU-1-3** series) displayed negligible activity to inhibit

cholinesterase enzymes in comparison to the activities of the title urolithin amides. This implies the significance of terminal nitrogen substitution to obtain cholinesterase inhibitor agents within the design employed.

It is well known that the coumarin scaffold itself provides MAO inhibition, as it is observed in many synthetic and natural coumarin and flavonoid analogs.<sup>[27]</sup> As seen in Table 1, although both synthesis intermediates and the title urolithin amides were found to possess MAO-B inhibitory potential within the IC<sub>50</sub> range of 12–42 μM, none of them were found superior to the activity obtained with the reference molecule pargyline.

The synthesis intermediates of both URO and THU derivatives were found to possess the weakest activities. This means that the URO- (or THU)-spacer-amide scaffold was proven to be an effective strategy within the design of dual cholinesterase and MAO-B inhibitor molecules. In general, the title THU derivatives displayed a more inhibitory activity in comparison to their URO analogs. Among the title amides, **THU-8** and **URO-8** were observed to be the most potent inhibitor compounds, respectively. The propargyl group is present as the common point in the structural organization of these molecules. Once considered that *N*-propargyl substitution has effectively been employed in the design of MAO-B inhibitor drugs (e.g., pargyline, selegiline, and rasagiline), it is possible to postulate that the propargyl moiety in these compounds also aided in increasing the potential of the compounds to act as MAO-B inhibitors.<sup>[28]</sup> Besides, the carbohydrazide derivatives **THU-9** and **URO-9** also displayed promising MAO-B inhibitor activities among other test materials. This has also been found as an important outcome regarding the structure of an MAO inhibitor drug, isocarboxazid, a carbohydrazide analog.<sup>[29]</sup>

### 2.3 | Docking studies

To gain insight into the predicted binding modes of the most active compounds, docking studies were performed. Figure 2 shows the predicted binding modes of compound **THU-4** at the AChE (Figure 2a) and BuChE (Figure 2b) binding sites. The docking studies suggested binding modes in which the tetrahydrourolithin scaffold is situated at the peripheral site of the pocket, whereas the benzyl group is accommodated in the catalytic active site. The inhibitor binding is stabilized by different interactions. Specifically, at the AChE binding site, **THU-4** establishes a hydrogen bond with the backbone carbonyl of Phe295 and π-π stacking interactions with Tyr341. The benzyl group interacts with Trp86 through hydrophobic contacts. At the BuChE binding site, instead, hydrogen bonds are formed with Ser198 and His438, whereas π-π stacking interactions are observed between the core of **THU-4** and Phe329 and the benzyl group and Trp82.

According to our computational studies, **THU-8** forms a hydrogen bond with Tyr435 and several hydrophobic interactions with the surrounding residues, which stabilize the compound at the hMAO-B pocket. The predicted binding mode of compound **THU-8** is shown in Figure 3.

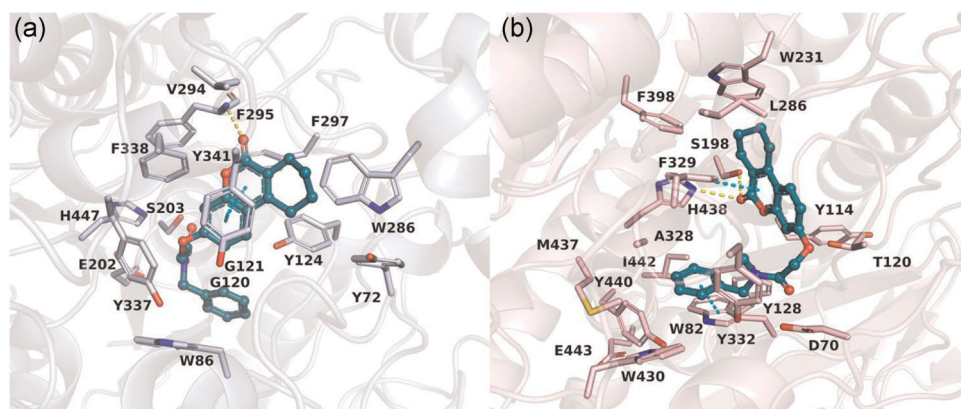


**FIGURE 2** Docking poses of compound **THU-4** at the binding site of hAChE (a) and hBuChE (b). PDB IDs: 6O4W and 6F7Q. The side chains of the amino acids surrounding the ligand are shown as white sticks (hAChE) and pink sticks (hBuChE); for residue F295 (hAChE), the main chain is displayed. Hydrogen bond interactions are illustrated with dashed yellow lines, whereas  $\pi$ - $\pi$  stacking interactions are shown with dashed cyan lines. The docking poses are shown by a ball-and-stick representation, with dark cyan color. AChE, acetylcholinesterase; BuChE, butyrylcholinesterase

## 2.4 | The potential of the compounds to inhibit A $\beta$ aggregation

It is well known that the deposition of A $\beta$  aggregates is involved in the pathogenesis of AD. Many studies have indicated the activation of cascades through this A $\beta$  toxicity. Therefore, the prevention of A $\beta$  aggregates is one of the strategies followed in the MTLA approach for the treatment of AD.<sup>[4,5]</sup>

In this study, the potential of the title compounds to inhibit A $\beta$  self-aggregation was also analyzed, and the results obtained are shown in Table 2. Accordingly, the results pointed out the moderate activity of the urolithin amides. In general, the percent inhibition at 100  $\mu$ M concentrations of the amide derivatives was within the range of 25–50%. The URO series was found more active in

comparison to the corresponding analogs within the THU series. The most active compound was **URO-7**, a naphthylamide compound. The activities were not found weaker in comparison to the reference molecule resveratrol. However, both THU and URO series displayed comparable/superior activities in comparison to the activity of donepezil, a selective AChE inhibitor, under the same experimental conditions. It is noteworthy to state that the synthesis intermediates (**URO-1–URO-3** and **THU-1–THU-3**) displayed weaker activities in comparison to the majority of the title compounds (i.e., the amide derivatives).

The results depicted that the design employed might be promising for the generation of more active compounds to prevent A $\beta$  aggregation. Previous studies on coumarin derivatives pointed out their A $\beta$  aggregation inhibitor potential.<sup>[30]</sup> Therefore, the results obtained

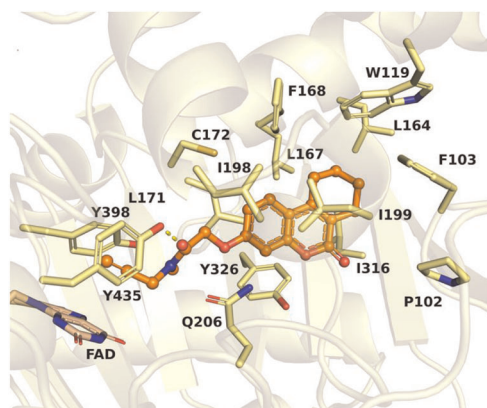


**FIGURE 3** Docking pose of compound **THU-8** at the hMAO-B active site. PDB ID: 6FVZ. The side chains of the amino acids surrounding the ligand are shown as yellow sticks, whereas FAD is shown as a beige stick. Hydrogen bond interaction is illustrated with a dashed yellow line. The docking pose is shown by a ball-and-stick representation, with an orange color. FAD, flavin adenine dinucleotide; MAO-B, monoamine oxidase B

**TABLE 2** The potential of the compounds to inhibit amyloid-beta aggregation<sup>a</sup>

URO series	% Inhibition	THU series	% Inhibition
<b>URO-1</b>	20.8 $\pm$ 1.2	<b>THU-1</b>	17.2 $\pm$ 1.4
<b>URO-2</b>	18.8 $\pm$ 1.6	<b>THU-2</b>	18.5 $\pm$ 2.9
<b>URO-3</b>	18.9 $\pm$ 1.4	<b>THU-3</b>	15.4 $\pm$ 1.1
<b>URO-4</b>	44.2 $\pm$ 0.9	<b>THU-4</b>	28.1 $\pm$ 1.9
<b>URO-5</b>	28.1 $\pm$ 2.9	<b>THU-5</b>	22.8 $\pm$ 1.4
<b>URO-6</b>	27.9 $\pm$ 0.8	<b>THU-6</b>	19.8 $\pm$ 3.1
<b>URO-7</b>	51.9 $\pm$ 1.4	<b>THU-7</b>	30.9 $\pm$ 1.8
<b>URO-8</b>	30.1 $\pm$ 1.0	<b>THU-8</b>	24.7 $\pm$ 0.5
<b>URO-9</b>	25.8 $\pm$ 1.5	<b>THU-9</b>	23.8 $\pm$ 1.7
<b>URO-10</b>	36.1 $\pm$ 2.0	<b>THU-10</b>	23.9 $\pm$ 2.0
Resveratrol	70.9 $\pm$ 0.55	Donepezil	26.1 $\pm$ 1.1

<sup>a</sup>Each compound was tested at 100  $\mu$ M.

for THU and URO series on the inhibition of aggregation of A $\beta$  also pointed out the significance of the coumarin structure and its eligibility to be improved with diverse modifications such as the employment of urolithin amide design present in the title compounds.

## 2.5 | The potential of the compounds to act as antioxidants

The antioxidant potential of the title compounds was screened employing the oxygen radical absorbance capacity (ORAC) test, a spectrofluorometric method. Trolox, a vitamin E analog, was used as a standard. The results are shown in Table 3.

Accordingly, the title molecules including the synthesis intermediates displayed ORAC-FL values around 3–4  $\mu$ M range Trolox equivalents. The activity of the title molecules was found slightly higher than the synthetic intermediates. Previous studies indicated that coumarin-based compounds display antioxidant activities in the ORAC assay.<sup>[31]</sup> Considering the fact that both URO and THU derivatives are coumarin analogs, the similar results obtained within the amide derivatives and synthesis intermediates might be attributed to the function of the coumarin system common in the design of the molecules.

## 3 | CONCLUSION

A series of urolithin analogs designed and synthesized within this study displayed varying inhibitory potential against cholinesterase enzymes and MAO-B. The docking studies with the most active compounds (THU-4 and THU-8, respectively, for cholinesterases and MAO-B) revealed the possible interactions with the enzymes. The title molecules, in general, also were shown to possess A $\beta$  inhibitor and antioxidant properties. Overall, the results depicted that the urolithin scaffold can be employed to design multitarget ligands for the treatment of AD. Regarding our previous studies on the design of cholinesterase inhibitor urolithin derivatives, this study further extrapolated the employment of urolithins to also act as MAO-B inhibitors concomitant to their cholinesterase inhibitor activities.

## 4 | EXPERIMENTAL

### 4.1 | Chemistry

#### 4.1.1 | General

The reagents and solvents employed in this study were obtained from local commercial suppliers. The reactions were monitored via thin-layer chromatography (TLC), performed on Merck aluminum-packed silica gel plates using ethyl acetate/cyclohexane as mobile phase (2:1 and 1:1 ratios). Mass spectral analysis was conducted on an Advion Expression CMS device. Samples are directly applied to the device via Atmospheric Solids Analysis Probe (ASAP) probe.

**TABLE 3** Antioxidant activity of the compounds

Title molecules (URO series)	ORAC ( $\mu$ mol Trolox equivalent/ $\mu$ mol of test compound)	Title molecules (THU series)	ORAC ( $\mu$ mol Trolox equivalent/ $\mu$ mol of test compound)
URO-1	4.2 $\pm$ 0.02	THU-1	4.7 $\pm$ 0.21
URO-2	4.0 $\pm$ 0.14	THU-2	4.4 $\pm$ 0.07
URO-3	4.7 $\pm$ 0.27	THU-3	4.3 $\pm$ 0.04
URO-4	3.3 $\pm$ 0.07	THU-4	3.7 $\pm$ 0.28
URO-5	3.7 $\pm$ 0.10	THU-5	3.2 $\pm$ 0.15
URO-6	4.1 $\pm$ 0.21	THU-6	3.5 $\pm$ 0.24
URO-7	3.4 $\pm$ 0.11	THU-7	3.5 $\pm$ 0.04
URO-8	2.9 $\pm$ 0.16	THU-8	3.2 $\pm$ 0.19
URO-9	2.9 $\pm$ 0.32	THU-9	3.3 $\pm$ 0.07
URO-10	3.0 $\pm$ 0.08	THU-10	3.3 $\pm$ 0.28

Abbreviation: ORAC, oxygen radical absorbance capacity.

Scanning was completed in both negative and positive modes. The IR spectra of the compounds were obtained using a Shimadzu FT-IR Prestige model spectrophotometer. <sup>1</sup>H NMR (at 400 MHz) and <sup>13</sup>C NMR (at 100 MHz) spectra were recorded on a Bruker-400 NMR spectrometer using tetramethylsilane as an internal standard and dimethyl sulfoxide (DMSO; *d*<sub>6</sub>) as a solvent; all chemical shifts were reported in parts per million (ppm,  $\delta$ ). The elemental analysis was performed on a Thermo Fisher Scientific Model Flash Smart CHNS elemental analyzer.

The InChI codes of the investigated compounds, together with some biological activity data, are provided as Supporting Information.

#### 4.1.2 | Preparation of the synthesis intermediates

##### 3-Hydroxy-6H-benzo[c]chromen-6-one (URO-1)

The solution of 2-iodobenzoic acid (15 mmol) and resorcinol (45 mmol) in 30 ml of aqueous NaOH solution (55 mmol) was refluxed for 1 h. At the end of the time, CuSO<sub>4</sub> aqueous solution (2 g/10 ml) was added to the solution and the mixture was refluxed for additional 10 min. The precipitate formed was filtered and washed with acidified water. White-yellow powder, yield obtained 80%. IR: 1702 cm<sup>-1</sup> (lactone carbonyl). <sup>1</sup>H NMR (DMSO-*d*<sub>6</sub>, 400 MHz): 10.30 (s, 1H); 8.15–8.12 (m, 3H); 7.83 (t, 1H, *J* = 6.1); 7.50 (t, 1H, *J* = 6.1); 6.77–6.74 (m, 2H). <sup>13</sup>C NMR (DMSO-*d*<sub>6</sub>)  $\delta$  162.85, 159.21, 153.27, 135.80, 134.99, 131.07, 129.16, 124.72, 121.63, 121.18, 120.23, 112.90. MS: 212.9 (M–H<sup>+</sup>). Anal. calc. for C<sub>13</sub>H<sub>8</sub>O<sub>3</sub>: C, 73.58; H, 3.80. Found C, 73.69; H 3.76.

##### Ethyl 2-(6-oxo-6H-benzo[c]chromen-3-yloxy)acetate (URO-2)

Here, 10 mmol of URO-1 was dissolved in 30 ml of dimethylformamide; then, 15 mmol of NaH was added to this solution and the

mixture was stirred for 5 min. The reaction was started with the addition of 30 mmol of ethyl 2-chloroacetate. After running the reaction for 20 min at room temperature (rt), the mixture was poured into ice water. The precipitate formed was filtered and washed with water. Light brown powder, yield obtained 80%. IR: 1743  $\text{cm}^{-1}$  (aliphatic ester carbonyl), 1704  $\text{cm}^{-1}$  (lactone carbonyl).  $^1\text{H}$  NMR (DMSO- $d_6$ , 400 MHz): 8.37–8.20 (m, 3H); 7.80 (t, 1H,  $J = 6.0$ ); 7.66 (t, 1H,  $J = 6.0$ ); 7.07–6.93 (m, 2H); 4.89 (s, 2H); 4.19 (q, 2H,  $J = 7.1$  Hz); 1.26 (t, 3H,  $J = 7.1$  Hz).  $^{13}\text{C}$  NMR (DMSO- $d_6$ )  $\delta$  169.92, 159.25, 152.81, 136.04, 130.09, 129.67, 125.34, 124.85, 120.58, 114.47, 112.25, 103.90, 65.63, 61.44, 14.49. MS: 299.5 ( $\text{MH}^+$ ). Anal. calc. for  $\text{C}_{17}\text{H}_{14}\text{O}_5$ : C, 68.45; H, 4.73. Found C, 68.11; H, 4.68.

#### 2-(6-Oxo-6H-benzo[*c*]chromen-3-yloxy)acetic acid (URO-3)

Here, 10 mmol of **URO-2** was dissolved in the solution of KOH in methanol (1 g/30 ml) and the solution was refluxed for 2 h. At the end of this period followed by TLC studies, the reaction was cooled to rt and the organic solvent was evaporated under reduced pressure. The residue left was treated with water and the precipitate was filtered off and washed with water. White to light brown powder, yield obtained 89%. IR: 1727  $\text{cm}^{-1}$  (carboxylic acid carbonyl), 1700  $\text{cm}^{-1}$  (lactone carbonyl).  $^1\text{H}$  NMR (DMSO- $d_6$ , 400 MHz): 13.1 (bs, 1H); 8.32–8.17 (m, 3H); 7.89 (t, 1H,  $J = 6.0$ ); 7.60 (t, 1H,  $J = 6.0$ ); 7.10–6.90 (m, 2H); 4.75 (s, 2H).  $^{13}\text{C}$  NMR (DMSO- $d_6$ )  $\delta$  178.18, 161.27, 153.27, 135.36, 129.70, 128.23, 124.80, 122.05, 119.33, 111.14, 102.34, 88.82. MS: 269.4 ( $\text{M-H}^-$ ). Anal. calc. for  $\text{C}_{15}\text{H}_{10}\text{O}_5$ : C, 66.67; H, 3.73. Found C, 67.02; H, 3.71.

#### 7,8,9,10-Tetrahydro-3-hydroxybenzo[*c*]chromen-6-one (THU-1)

A mixture of resorcinol (90 mmol) and ethyl 2-oxocyclohexanecarboxylate (99.0 mmol) was heated at 75°C in the presence of  $\text{ZnCl}_4$  (50 mmol) for 1 h under neat conditions. The precipitate formed was filtered and washed with water. Yellow powder, yield obtained 87%. IR: 1737  $\text{cm}^{-1}$  (lactone carbonyl).  $^1\text{H}$  NMR (DMSO- $d_6$ , 400 MHz): 10.31 (bs, 1H); 7.50 (d, 1H,  $J = 8.8$ ); 6.75 (d, 1H,  $J = 8.8$ ); 6.65 (s, 1H); 2.71 (t, 2H,  $J = 5.6$ ); 2.48 (t, 2H,  $J = 6.0$ ); 1.73–1.67 (m, 4H).  $^{13}\text{C}$  NMR (DMSO- $d_6$ )  $\delta$  161.01, 153.03, 147.72, 125.05, 118.43, 112.67, 111.97, 101.91, 24.59, 23.47, 21.24, 20.87. MS: 216.8 ( $\text{M-H}^+$ ). Anal. calc. for  $\text{C}_{13}\text{H}_{12}\text{O}_3$ : C, 72.21; H, 5.59. Found C, 71.77; H, 5.70.

#### Ethyl 2-(7,8,9,10-tetrahydro-6-oxo-6H-benzo[*c*]chromen-3-yloxy)-acetate (THU-2)

The compound is synthesized according to the procedure provided for **URO-2**, except the employment of **THU-1** as the starting material. White powder, yield obtained 79%. IR: 1764  $\text{cm}^{-1}$  (aliphatic ester carbonyl), 1702  $\text{cm}^{-1}$  (lactone carbonyl).  $^1\text{H}$  NMR (DMSO- $d_6$ , 400 MHz): 7.60 (d, 1H,  $J = 9.6$ ); 6.94 (m, 2H); 4.88 (s, 2H); 4.15 (q, 2H,  $J = 7.2$  Hz); 2.74 (t, 2H,  $J = 6.0$  Hz); 2.37 (t, 2H,  $J = 5.2$  Hz); 1.71 (m, 4H); 1.19 (t, 3H,  $J = 7.2$ ).  $^{13}\text{C}$  NMR (DMSO- $d_6$ )  $\delta$  168.26, 160.79, 152.74, 147.45, 125.01, 119.79, 113.65, 112.11, 101.32, 64.89, 60.76, 24.61, 23.52, 21.15, 20.80, 14.02. MS: 303.6 ( $\text{MH}^+$ ). Anal. calc. for  $\text{C}_{17}\text{H}_{18}\text{O}_5$ : C, 67.54; H, 6.00. Found C, 67.44; H, 6.09.

#### 2-(7,8,9,10-Tetrahydro-6-oxo-6H-benzo[*c*]chromen-3-yloxy)acetic acid (THU-3)

The compound is synthesized according to the procedure provided for **URO-3**, except the employment of **THU-2** as the starting material. White powder, yield obtained 87%. IR: 1751  $\text{cm}^{-1}$  (aliphatic ester carbonyl), 1705  $\text{cm}^{-1}$  (lactone carbonyl).  $^1\text{H}$  NMR (DMSO- $d_6$ , 400 MHz): 7.63 (d, 1H,  $J = 8.8$ ); 6.95 (m, 2H); 4.80 (s, 2H); 2.77 (t, 2H,  $J = 5.6$  Hz); 2.40 (t, 2H,  $J = 5.2$  Hz); 1.75 (m, 4H).  $^{13}\text{C}$  NMR (DMSO- $d_6$ )  $\delta$  169.71, 160.82, 152.75, 147.49, 124.98, 119.66, 113.50, 112.08, 101.26, 64.77, 24.63, 23.53, 21.18, 20.82. MS: 273.5 ( $\text{M}^+$ ). Anal. calc. for  $\text{C}_{15}\text{H}_{14}\text{O}_5$ : C, 65.69; H, 5.15. Found C, 66.01; H, 4.99.

### 4.1.3 | General procedure for the synthesis of urolithin amides

**URO-3** and **THU-3** are employed as starting materials for the synthesis of the amide derivatives URO and THU series. Accordingly, the corresponding acetic acid derivative (2.3 mmol, either **URO-3** or **THU-3**) is dissolved in 30 ml of dichloromethane. Next, 2.3 mmol of thionyl chloride is added to the mixture and refluxed for 6 h. The mixture was evaporated under reduced pressure. The residue was added to 20 ml of dichloromethane. This solution was placed in an ice bath (0°C). The appropriate amine derivative (2.3 mmol) was added dropwise in 20 ml of dichloromethane. Then, the organic solvent was evaporated and the residue left was purified employing column chromatography (ethyl acetate/*n*-hexane 3:1, as the mobile phase).

#### 2-(6-Oxo-6H-benzo[*c*]chromen-3-yloxy)-*N*-benzyl-*N*-methylacetamide (URO-4)

Yellow powder, yield obtained 63%. IR: 1727  $\text{cm}^{-1}$  (lactone carbonyl), 1643  $\text{cm}^{-1}$  (amide carbonyl).  $^1\text{H}$  NMR (DMSO- $d_6$ , 400 MHz): 8.36–8.21 (m, 3H); 7.92 (t, 1H,  $J = 7.6$ ); 7.61 (t, 1H,  $J = 6.8$ ); 7.42 (t, 1H,  $J = 6.8$ ); 7.34–7.23 (m, 4H); 7.04 (t, 1H,  $J = 7.2$ ); 5.10 (s, 2H); 4.54 (s, 2H); 2.98 (s, 3H).  $^{13}\text{C}$  NMR (DMSO- $d_6$ )  $\delta$  168.14, 161.24, 155.05, 138.27, 135.68, 130.28, 125.41, 123.50, 119.52, 112.09, 110.8, 104.63, 66.98, 65.70, 54.14, 51.58. MS: 274.6 ( $\text{MH}^+$ ). Anal. calc. for  $\text{C}_{23}\text{H}_{19}\text{NO}_4$ : C, 73.98; H, 5.13; N, 3.75. Found C, 73.99; H, 4.99; N, 3.81.

#### 3-(2-Morpholino-2-oxoethoxy)-6H-benzo[*c*]chromen-6-one (URO-5)

Light yellow powder, yield obtained 58%. IR: 1727  $\text{cm}^{-1}$  (lactone carbonyl), 1654  $\text{cm}^{-1}$  (amide carbonyl).  $^1\text{H}$  NMR (DMSO- $d_6$ , 400 MHz): 8.35 (d, 1H,  $J = 8.6$ ); 8.01–7.95 (m, 2H); 7.80 (t, 1H,  $J = 6.8$ ); 7.52 (t, 1H,  $J = 6.8$ ); 7.01 (d, 1H,  $J = 8.8$ ); 6.89 (d, 1H,  $J = 2.4$ ); 4.78 (s, 2H); 3.71–3.57 (m, 4H).  $^{13}\text{C}$  NMR (DMSO- $d_6$ )  $\delta$  165.68, 159.24, 152.46, 134.94, 134.84, 130.59, 128.06, 124.09, 121.17, 120.12, 112.41, 112.21, 102.83, 77.01, 67.40, 66.80, 66.64, 45.76, 42.43. MS: 340.6 ( $\text{MH}^+$ ). Anal. calc. for  $\text{C}_{19}\text{H}_{17}\text{NO}_5$ : C, 67.25; H, 5.05; N, 4.13. Found C, 67.61; H, 4.88; N, 4.11.

#### 3-[2-(4-Benzylpiperazin-1-yl)-2-oxoethoxy]-6H-benzo[*c*]chromen-6-one (URO-6)

White powder, yield obtained 55%. IR: 1721  $\text{cm}^{-1}$  (lactone carbonyl), 1649  $\text{cm}^{-1}$  (amide carbonyl).  $^1\text{H}$  NMR (DMSO- $d_6$ , 400 MHz): 8.46–8.24

(m, 3H); 7.88 (t, 1H,  $J = 7.6$ ); 7.65 (t, 1H,  $J = 6.8$ ); 7.37–7.24 (m, 5H), 7.02 (t, 1H,  $J = 7.2$ ); 4.97 (s, 2H); 3.44 (s, 2H); 2.70–2.59 (m, 8H).  $^{13}\text{C}$  NMR (DMSO- $d_6$ )  $\delta$  165.81, 160.93, 153.41, 138.80, 136.25, 135.49, 130.73, 129.05, 128.08, 126.65, 125.18, 119.42, 112.51, 111.27, 103.68, 66.04, 62.72, 53.19, 43.71, 42.55. MS: 429.2 ( $\text{MH}^+$ ). Anal. calc. for  $\text{C}_{26}\text{H}_{24}\text{N}_2\text{O}_4$ : C, 72.88; H, 5.65; N, 6.54. Found C, 73.41; H, 5.90; N, 6.49.

*2-(6-Oxo-6H-benzo[*c*]chromen-3-yloxy)-N-(naphthalen-1-yl)-acetamide (URO-7)*

Yellowish powder, yield obtained 60%. IR: 1718  $\text{cm}^{-1}$  (lactone carbonyl), 1630  $\text{cm}^{-1}$  (amide carbonyl).  $^1\text{H}$  NMR (DMSO- $d_6$ , 400 MHz): 10.05 (s, 1H); 8.30–8.18 (m, 3H); 7.85–7.34 (m, 8H); 6.82–6.75 (m, 3H); 5.06 (s, 2H).  $^{13}\text{C}$  NMR (DMSO- $d_6$ )  $\delta$  167.09, 161.88, 155.25, 145.78, 137.28, 134.07, 133.39, 131.48, 127.89, 126.19, 125.61, 124.26, 123.82, 117.51, 106.79, 102.60, 67.81. MS: 396.10 ( $\text{MH}^+$ ). Anal. calc. for  $\text{C}_{25}\text{H}_{17}\text{NO}_4$ : C, 75.94; H, 4.33; N, 3.54. Found C, 76.12; H, 4.36; N, 3.47.

*2-(6-Oxo-6H-benzo[*c*]chromen-3-yloxy)-N-methyl-N-(prop-2-ynyl)-acetamide (URO-8)*

Brown powder, yield obtained 51%. IR: 1719  $\text{cm}^{-1}$  (lactone carbonyl), 1668  $\text{cm}^{-1}$  (amide carbonyl).  $^1\text{H}$  NMR (DMSO- $d_6$ , 400 MHz): 8.33–8.18 (m, 3H); 7.89 (t, 1H,  $J = 7.2$ ); 7.59 (t, 1H,  $J = 7.2$ ); 7.00–6.91 (m, 2H); 5.00 (s, 2H); 3.02 (s, 2H); 2.89 (s, 3H); 2.08 (s, 1H).  $^{13}\text{C}$  NMR (DMSO- $d_6$ )  $\delta$  166.69, 160.06, 151.91, 135.40, 134.77, 129.73, 128.22, 124.64, 122.05, 112.91, 102.33, 74.38, 65.67, 40.11, 35.82. MS: 322.0 ( $\text{MH}^+$ ). Anal. calc. for  $\text{C}_{19}\text{H}_{15}\text{NO}_4$ : C, 71.02; H, 4.71; N, 4.36. Found C, 71.28; H, 4.70; N, 4.33.

*2-(6-Oxo-6H-benzo[*c*]chromen-3-yloxy)-N'-phenylacetohydrazide (URO-9)*

Yellow powder, yield obtained 48%. IR: 1719  $\text{cm}^{-1}$  (lactone carbonyl), 1641  $\text{cm}^{-1}$  (amide carbonyl).  $^1\text{H}$  NMR (DMSO- $d_6$ , 400 MHz): 11.01 (s, 1H); 10.05 (s, 1H); 8.30–8.22 (m, 3H); 7.89 (t, 1H,  $J = 7.2$ ); 7.59 (t, 1H,  $J = 7.2$ ); 7.11–6.91 (m, 7H); 5.07 (s, 2H).  $^{13}\text{C}$  NMR (DMSO- $d_6$ ):  $\delta$  168.80, 160.54, 154.27, 137.93, 135.49, 134.85, 129.27, 128.64, 125.73, 123.86, 122.48, 119.82, 112.81, 111.48, 102.66, 67.49. MS: 361.0 ( $\text{MH}^+$ ). Anal. calc. for  $\text{C}_{21}\text{H}_{16}\text{N}_2\text{O}_4$ : C, 69.99; H, 4.48; N, 7.77. Found C, 70.48; H, 4.74; N, 7.60.

*3-[2-(3,4-Dihydro-6,7-dimethoxyisoquinolin-2(1H)-yl)-2-oxoethoxy]-6H-benzo[*c*]chromen-6-one (URO-10)*

Brown-yellow powder, yield obtained 58%. IR: 1724  $\text{cm}^{-1}$  (lactone carbonyl), 1665  $\text{cm}^{-1}$  (amide carbonyl).  $^1\text{H}$  NMR (DMSO- $d_6$ , 400 MHz): 8.31–8.17 (m, 3H); 7.89 (t, 1H,  $J = 7.2$ ); 7.58 (t, 1H,  $J = 7.6$ ); 7.03–6.99 (m, 2H); 6.80–6.72 (m, 2H); 5.04 (s, 2H); 3.72–3.63 (m, 10H); 3.27–3.17 (m, 2H).  $^{13}\text{C}$  NMR (DMSO- $d_6$ )  $\delta$  166.22, 160.47, 151.90, 147.46, 135.36, 134.68, 129.69, 128.16, 126.01, 124.70, 122.01, 119.27, 112.82, 102.33, 66.24, 55.51, 44.85. MS: 446.01 ( $\text{MH}^+$ ). Anal. calc. for  $\text{C}_{26}\text{H}_{23}\text{NO}_6$ : C, 70.10; H, 5.20; N, 3.14. Found C, 70.14; H, 5.12; N, 3.21.

*2-(7,8,9,10-Tetrahydro-6-oxo-6H-benzo[*c*]chromen-3-yloxy)-N-benzyl-N-methylacetamide (THU-4)*

White powder, yield obtained 68%. IR: 1700  $\text{cm}^{-1}$  (lactone carbonyl), 1676  $\text{cm}^{-1}$  (amide carbonyl).  $^1\text{H}$  NMR (DMSO- $d_6$ , 400 MHz): 7.48–7.18 (m, 6H); 6.85 (d, 1H,  $J = 9$ ); 6.67 (d, 1H,  $J = 9$ ); 4.81 (s, 2H); 4.60 (s, 2H); 2.99 (s, 3H); 2.74 (t, 2H,  $J = 5.8$ ); 2.56 (t, 2H,  $J = 5.8$ ); 1.86–1.78 (m, 4H).  $^{13}\text{C}$  NMR (DMSO- $d_6$ )  $\delta$  167.36, 160.01, 153.30, 147.17, 136.46, 135.83, 129.08, 128.70, 127.67, 126.43, 121.01, 114.52, 112.26, 66.90, 52.78, 51.24, 34.22. MS: 378.1 ( $\text{MH}^+$ ). Anal. calc. for  $\text{C}_{23}\text{H}_{23}\text{NO}_4$ : C, 73.19; H, 6.14; N, 3.71. Found C, 72.80; H, 6.22; N, 3.56.

*3-(2-Morpholino-2-oxoethoxy)-7,8,9,10-tetrahydrobenzo[*c*]chromen-6-one (THU-5)*

White powder, yield obtained 71%. IR: 1694  $\text{cm}^{-1}$  (lactone carbonyl), 1651  $\text{cm}^{-1}$  (amide carbonyl).  $^1\text{H}$  NMR (DMSO- $d_6$ , 400 MHz): 7.48 (d, 1H,  $J = 8.8$ ); 6.92 (d, 1H,  $J = 8.8$ ); 6.82 (d, 1H,  $J = 2.8$ ); 4.76 (s, 2H); 3.70–3.56 (m, 4H); 2.74 (t, 2H,  $J = 9.6$ ); 2.56 (t, 2H,  $J = 8.0$ ); 1.87–1.78 (m, 4H).  $^{13}\text{C}$  NMR (DMSO- $d_6$ )  $\delta$  165.66, 159.36, 153.32, 147.06, 124.44, 121.23, 114.70, 111.88, 101.79, 67.33, 66.63, 45.73, 42.40, 29.69, 25.22. MS: 344.1 ( $\text{MH}^+$ ). Anal. calc. for  $\text{C}_{19}\text{H}_{21}\text{NO}_5$ : C, 66.46; H, 6.16; N, 4.08. Found C, 66.74; H, 6.14; N, 4.01.

*3-[2-(4-Benzylpiperazin-1-yl)-2-oxoethoxy]-7,8,9,10-tetrahydrobenzo[*c*]chromen-6-one (THU-6)*

White powder, yield obtained 63%. IR: 1700  $\text{cm}^{-1}$  (lactone carbonyl), 1654  $\text{cm}^{-1}$  (amide carbonyl).  $^1\text{H}$  NMR (DMSO- $d_6$ , 400 MHz): 7.43 (d, 1H,  $J = 8.8$ ); 7.30–7.25 (m, 5H); 6.89 (d, 1H,  $J = 9.0$ ); 6.77 (d, 1H,  $J = 2.4$ ); 4.75 (s, 2H); 3.51 (s, 2H); 2.71 (t, 2H,  $J = 9.6$ ); 2.52 (t, 2H,  $J = 8.0$ ); 2.44–2.40 (m, 4H); 1.83–1.77 (m, 4H).  $^{13}\text{C}$  NMR (DMSO- $d_6$ )  $\delta$  165.37, 159.57, 153.20, 147.15, 137.39, 129.01, 128.32, 127.29, 124.32, 120.87, 114.42, 111.97, 101.72, 67.12, 62.72, 52.54, 45.09, 42.06, 29.26, 25.15, 23.82. MS: 432.2 ( $\text{M}^+$ ). Anal. calc. for  $\text{C}_{26}\text{H}_{28}\text{N}_2\text{O}_4$ : C, 72.20; H, 6.53; N, 6.48. Found C, 71.88; H, 6.39; N, 6.57.

*2-(7,8,9,10-Tetrahydro-6-oxo-6H-benzo[*c*]chromen-3-yloxy)-N-(naphthalen-1-yl)acetamide (THU-7)*

Light yellow powder, yield obtained 58%. IR: 1705  $\text{cm}^{-1}$  (lactone carbonyl), 1662  $\text{cm}^{-1}$  (amide carbonyl).  $^1\text{H}$  NMR (DMSO- $d_6$ , 400 MHz): 10.33 (s, 1H); 7.50–7.14 (m, 8H); 6.95 (d, 1H,  $J = 9.0$ ); 6.73 (d, 1H,  $J = 2.8$ ); 5.01 (s, 2H); 2.73 (t, 2H,  $J = 5.6$ ); 2.44 (t, 2H,  $J = 5.6$ ); 1.71–1.66 (m, 4H).  $^{13}\text{C}$  NMR (DMSO- $d_6$ )  $\delta$  167.01, 160.39, 154.41, 147.26, 145.28, 134.83, 132.91, 128.52, 127.26, 126.45, 124.06, 123.62, 120.07, 116.55, 114.93, 112.84, 108.41, 103.86, 68.35, 26.21, 25.09, 22.27. MS: 400.2 ( $\text{MH}^+$ ). Anal. calc. for  $\text{C}_{25}\text{H}_{21}\text{NO}_4$ : C, 75.17; H, 5.30; N, 3.51. Found C, 75.41; H, 5.20; N, 3.39.

*2-(7,8,9,10-Tetrahydro-6-oxo-6H-benzo[*c*]chromen-3-yloxy)-N-methyl-N-(prop-2-ynyl)acetamide (THU-8)*

White powder, yield obtained 58%. IR: 1695  $\text{cm}^{-1}$  (lactone carbonyl), 1670  $\text{cm}^{-1}$  (amide carbonyl).  $^1\text{H}$  NMR (DMSO- $d_6$ , 400 MHz): 7.47 (d, 1H,  $J = 8.8$ ); 6.92 (d, 1H,  $J = 9.0$ ); 6.78 (d, 1H,  $J = 2.4$ ); 4.76 (s, 2H);

3.21 (s, 2H); 3.04 (s, 3H); 2.74 (t, 2H,  $J = 5.2$ ); 2.55 (t, 2H,  $J = 5.2$ ); 2.37 (s, 1H); 1.85–1.60 (m, 4H).  $^{13}\text{C}$  NMR (DMSO- $d_6$ )  $\delta$  166.68, 159.53, 153.27, 144.16, 124.36, 121.08, 112.20, 112.07, 101.90, 72.50, 66.77, 38.74, 36.63, 33.49, 25.21, 23.83, 21.70, 21.33. MS: 326.1 (MH $^+$ ). Anal. calc. for C $_{19}$ H $_{19}$ NO $_4$ : C, 70.14; H, 5.89; N, 4.31. Found C, 70.01; H, 5.88; N, 4.39.

*2-(7,8,9,10-Tetrahydro-6-oxo-6H-benzo[c]chromen-3-yloxy)-N'-phenylacetohydrazide (THU-9)*

White powder, yield obtained 58%. IR: 1695 cm $^{-1}$  (lactone carbonyl), 1670 cm $^{-1}$  (amide carbonyl).  $^1\text{H}$  NMR (DMSO- $d_6$ , 400 MHz): 7.53 (d, 1H,  $J = 8.8$ ); 7.26–7.19 (m, 2H); 6.95–6.84 (m, 5H); 4.69 (s, 2H); 2.75 (t, 2H,  $J = 5.6$ ); 2.54 (t, 2H,  $J = 5.6$ ); 1.88–1.63 (m, 4H).  $^{13}\text{C}$  NMR (DMSO- $d_6$ )  $\delta$  167.18, 161.77, 153.33, 147.34, 146.93, 129.25, 124.67, 121.75, 121.66, 115.23, 113.72, 112.56, 111.34, 110.00, 102.23, 77.01, 67.20, 29.69, 25.24, 23.88, 21.57, 21.30. MS: 365.2 (MH $^+$ ). Anal. calc. for C $_{21}$ H $_{20}$ N $_2$ O $_4$ : C, 69.22; H, 5.53; N, 7.69. Found C, 69.58; H, 5.58; N, 7.80.

*3-[2-(3,4-Dihydro-6,7-dimethoxyisoquinolin-2(1H)-yl)-2-oxoethoxy]-7,8,9,10-tetrahydrobenzo[c]chromen-6-one (THU-10)*

Light yellow powder, yield obtained 71%. IR: 1695 cm $^{-1}$  (lactone carbonyl), 1673 cm $^{-1}$  (amide carbonyl).  $^1\text{H}$  NMR (DMSO- $d_6$ , 400 MHz): 7.46 (d, 1H,  $J = 8.8$ ); 6.95 (d, 1H,  $J = 8.8$ ); 6.83 (s, 1H); 6.63–6.58 (m, 2H); 4.83 (s, 2H); 4.67 (s, 2H); 3.86 (s, 3H); 3.80 (s, 3H); 3.74 (t, 2H,  $J = 6$ ); 2.85 (t, 2H,  $J = 6$ ); 2.72 (t, 2H,  $J = 5.6$ ); 2.54 (t, 2H,  $J = 5.6$ ); 1.85–1.77 (m, 4H).  $^{13}\text{C}$  NMR (DMSO- $d_6$ )  $\delta$  166.01, 161.96, 153.30, 147.94, 147.11, 126.58, 125.39, 124.43, 123.48, 121.11, 114.62, 112.12, 111.78, 111.17, 109.25, 108.72, 101.82, 67.64, 55.95, 46.43, 44.27, 43.09, 40.33, 29.01, 25.20, 23.84, 21.63. MS: 450.2 (MH $^+$ ). Anal. calc. for C $_{26}$ H $_{27}$ NO $_6$ : C, 69.47; H, 6.05; N, 3.12. Found C, 69.75; H, 5.99; N, 3.20.

## 4.2 | Biological evaluation

### 4.2.1 | Cholinesterase inhibition assays

To screen the potential of the title molecules and synthesis intermediates (i.e., **URO-1–10** and **THU-1–10**) to inhibit AChE and BuChE, modified Ellmann's method was employed.<sup>[15,18]</sup> Each enzyme assay was performed in 50 mM Tris-HCl buffer (pH 8.0), containing 6.8 mM DTNB solution, 20 mM MgCl $_2$ , 100 mM NaCl, and 10  $\mu\text{l}$  of AChE or BuChE solution (0.4 U/ml from human recombinant AChE or 1.64 U/ml from human recombinant BuChE, from Sigma-Aldrich), and 2  $\mu\text{l}$  of each sample solution in a total volume of 190  $\mu\text{l}$ . Depending on the enzyme used, either 10  $\mu\text{l}$  of 10 mM acetylthiocholine iodide solution or 10  $\mu\text{l}$  of 1.5 mM butyrylthiocholine iodide solution was added to initiate the enzyme-catalyzed reactions. In the control group, representing the full activity, no inhibitor was used. UV measurements were performed at 412 nm, employing a 96-well microplate reader (i.e., Varioskan Flash; Thermo Fisher Scientific) immediately after the

incubation time (15 min) at 27°C. The percent inhibition of test compounds was calculated via the formula  $(\text{FA} - \text{IA})/\text{FA} \times 100$ , where FA represents the full activity obtained in the absence of inhibitor and IA is the activity obtained in the presence of an inhibitor (i.e., test or reference compound). The IC $_{50}$  values for AChE and BuChE were calculated by plotting the percent inhibition against the concentration of test materials. Each experiment was run in triplicate and the results were represented as mean  $\pm$  SD. Rivastigmine and donepezil were used as standard inhibitors for both cholinesterases.

### 4.2.2 | MAO-B inhibition assays

An MAO assay kit (i.e., Sigma-Aldrich Monoamine Oxidase Assay Kit, Catalog Number: MAK-136) was employed to measure the potential of the title amide derivatives and synthesis intermediates to inhibit MAO-B.<sup>[18]</sup> Accordingly, *p*-tyramine was employed as the substrate of the reaction, and the MAO-B-catalyzed formation of hydrogen peroxide was measured employing a dye reagent through a fluorescence assay in which excitation and emission wavelengths were set to 530 and 585 nm, respectively. In full activity tests, no inhibitor was employed. Assays were performed in triplicate and the percent inhibition was plotted against concentration to obtain IC $_{50}$ s. Pargyline was employed as the reference inhibitor as provided within the kit. The mean  $\pm$  SD of IC $_{50}$  values obtained was presented.

### 4.2.3 | Inhibition of A $\beta$ aggregation

The thioflavin T fluorescence spectroscopy method was employed to screen the potential of the molecules to inhibit amyloid beta (A $\beta$  $_{1-42}$  from Sigma-Aldrich) self-aggregation.<sup>[16]</sup> Briefly, for the preparation of A $\beta$ , 1 mg was dissolved in 0.5 ml of hexafluoroisopropanol (HFIP). Then, HFIP was evaporated and 2.3 mM A $\beta$  stock solution was prepared in DMSO, and 2  $\mu\text{l}$  of this solution was transferred to each well of a 24-well multidish microplate. Each well was further added with 18  $\mu\text{l}$  of 0.2 M sodium phosphate buffer (pH 8.0) containing either title molecules or reference compounds (i.e., resveratrol). The final solutions were incubated for 36 h at rt. After the incubation time, 1.5  $\mu\text{M}$  thioflavin T solution in 50 mM glycine-NaOH buffer (pH 8.5) was added to generate a total volume of 2 ml. Fluorescence analysis through a Varioskan Flash Thermo Scientific instrument was performed with excitation and emission wavelengths set to 446 and 490 nm, respectively. Each experiment was run in triplicate and percent inhibition results were presented as mean  $\pm$  SD. In control experiments, no reference or test compounds were employed. Both the test compounds and standards were employed at 100  $\mu\text{M}$  final concentration. The formula  $100 - (\text{IFI}/\text{IFo}) \times 100$  was used to calculate the potential of the test compounds to prevent A $\beta$  aggregation. In the formula, IFI and IFo represent the fluorescence intensities obtained in the presence and absence of test/reference compounds used.

#### 4.2.4 | Antioxidant assays

The ORAC test was employed to determine the antioxidant activity of the compounds.<sup>[32]</sup> Accordingly, assays were performed in 200  $\mu$ l volume of 75 mM phosphate buffer at pH 7.4. Next, 20  $\mu$ l of test substances (final 10  $\mu$ M concentration) and 120  $\mu$ l of fluorescein (150 nM final concentration) were incubated for 20 min at 37°C. After the incubation time, 60  $\mu$ l of 2,2'-azobis(2-methylpropionamide) dihydrochloride (12 mM final concentration) was added to each solution well. Measurements were performed through recording fluorescence readings (i.e., excitation at 485 nm and emission at 535 nm in a Thermo Scientific Varioskan Flash Multimode Reader) at 5-min intervals for 90 min. Also, 0.5–8  $\mu$ M final concentrations of Trolox were used as standards. Each assay was done in triplicate. The ORAC values, calculated as the difference of the areas under the quenching curves of fluoresceine between the blank and the sample, were expressed as  $\mu$ mol Trolox equivalents per  $\mu$ mol of compounds.

#### 4.3 | Docking studies

Docking studies were carried out with Schrödinger suite 2018-1 using the same protocol implemented in our previous study.<sup>[18,33]</sup> In particular, the crystal structures of hAChE (PDB ID: 6O4W), hBuChE (PDB ID: 6F7Q), and hMAO-B (PDB ID: 6FVZ) were downloaded from the Protein Data Bank (PDB) and prepared with Schrödinger's Protein Preparation Wizard tool.<sup>[34–38]</sup> Water molecules and residues defined as heteroatoms in PDB were removed, except FAD in the crystal structure of MAO-B (PDB ID: 6FVZ). During the protein preparation step, hydrogen atoms and missing side-chain residues were added; then, residues protonation states were predicted by PROPKA at pH 7.0 and the hydrogen bonding network was optimized. As a final step, the proteins were subjected to a restrained energy minimization using the OPLS3 force field with default settings. The ligand structures under investigation were prepared by means of Schrödinger's LigPrep tool with the following settings: stereoisomers generated at pH 7.0  $\pm$  2.0 with Epik, possible tautomers generation, OPLS3 as force field.<sup>[39]</sup> Afterward, a maximum of 25 conformers were generated for each ligand using ConfGen and the outputs were minimized with OLPS\_2005 force field (default force field).<sup>[40,41]</sup> To dock our inhibitors at the relative binding pocket, grid boxes were generated using the Receptor Grid Generation tool. The co-crystallized inhibitor of each protein was selected as the center of the grid. Molecular docking studies were performed with Glide Standard Precision (SP) mode from the Schrödinger suite. The option "sample ring conformation" was turned on and a maximum of three docking poses was output for each ligand.<sup>[42]</sup> Subsequently, the first poses were refined and minimized using protein–ligand complex refinement, allowing flexibility for the residues within 2 Å from the ligand; VSGB and OPLS3 were used as solvation model and force field, respectively.<sup>[43]</sup> The implemented protocol was first tested via redocking studies to check the ability to reproduce the co-crystallized inhibitor structures. In all three cases,

low root-mean-square deviation (RMSD) values were obtained: 6O4W = 0.836 Å, 6F7Q = 0.631 Å, 6FVZ = 0.109 Å (RMSD of heavy atoms).

#### CONFLICTS OF INTERESTS

The authors declare that there are no conflicts of interests.

#### ORCID

Hayrettin O. Gulcan  <http://orcid.org/0000-0002-9503-5841>

#### REFERENCES

- [1] G. Sarıkaya, G. Coban, S. Parlar, A. H. Tarikogullari, G. Armagan, M. A. Erdogan, V. Alptüzün, A. S. Alpan, *Arch. Pharm.* **2018**, *351*, e1800076.
- [2] Alzheimer's Association, *Alzheimer's Dementia* **2019**, *15*, 321.
- [3] T. Gabriella, E. Staurengi, C. Zerbinati, S. Gargiulo, L. Iuliano, G. Giaccone, F. Fantò, G. Poli, G. Leonarduzzi, P. Gamba, *Redox Biol.* **2016**, *10*, 24.
- [4] H. O. Gulcan, I. E. Orhan, *Pharmaceutical Biocatalysis: Fundamentals, Enzyme Inhibitors, and Enzymes in Health and Diseases* (Ed: P. Grunwald), Jenny Stanford Publishing, New York, NY **2019**, Ch. 12.
- [5] B. Kılıç, H. O. Gulcan, F. Aksakal, T. Ercetin, N. Oruklu, E. U. Bagriacik, D. S. Dogruer, *Bioorg. Chem.* **2018**, *79*, 235.
- [6] M. Rossor, L. L. Iversen, *Br. Med. Bull.* **1986**, *42*, 70.
- [7] M. J. West, P. D. Coleman, D. G. Flood, J. C. Troncoso, *Lancet* **1994**, *344*, 769.
- [8] D. R. Gitelman, I. Prohovnik, *Neurobiol. Aging* **1992**, *13*, 313.
- [9] R. Raschetti, E. Albanese, N. Vanacore, M. Maggini, *PLOS Med.* **2007**, *4*, e338.
- [10] B. Reisberg, R. Doody, A. Stöffler, F. Schmitt, S. Ferris, H. J. Möbius, *N. Engl. J. Med.* **2003**, *348*, 1333.
- [11] F. Mesiti, D. Chavarria, A. Gaspar, S. Alcaro, F. Borges, *Eur. J. Med. Chem.* **2019**, *181*, 111572.
- [12] H. O. Gulcan, A. Mavideniz, M. F. Sahin, I. E. Orhan, *Curr. Med. Chem.* **2019**, *26*, 3260.
- [13] C. R. Jack Jr, D. S. Knopman, W. J. Jagust, R. C. Petersen, M. W. Weiner, P. S. Aisen, L. M. Shaw, P. Vemuri, H. J. Wiste, S. D. Weigand, T. G. Lesnick, *Lancet Neurol.* **2013**, *12*, 207.
- [14] F. J. Pérez-Areales, M. Garrido, E. Aso, M. Bartolini, A. De Simone, A. Espargaró, T. Ginex, R. Sabate, B. Pérez, V. Andrisano, D. Puigoriol-Illamola, *J. Med. Chem.* **2020**, *63*, 9360.
- [15] H. O. Gulcan, S. Unlu, I. Esiringu, T. Ercetin, Y. Sahin, D. Oz, M. F. Sahin, *Bioorg. Med. Chem.* **2014**, *22*, 5141.
- [16] M. Norouzbahari, E. V. Burgaz, T. Ercetin, A. Fallah, A. Foroumadi, L. Firoozpour, M. F. Sahin, M. Gazi, H. O. Gulcan, *Lett. Drug Des. Discov.* **2018**, *15*, 1131.
- [17] F. A. Tomás-Barberán, A. González-Sarriás, R. García-Villalba, M. A. Núñez-Sánchez, M. V. Selma, M. T. García-Conesa, J. C. Espín, *Mol. Nutr. Food Res.* **2017**, *61*, 1500901.
- [18] B. Noshadi, T. Ercetin, C. Luise, M. Y. Yuksel, W. Sippl, M. F. Sahin, M. Gazi, H. O. Gulcan, *Chem. Biodivers.* **2020**, *17*, e2000197.
- [19] A. Samadi, M. Chioua, I. Bolea, C. de los Ríos, I. Iriepa, I. Moraleda, A. Bastida, G. Esteban, M. Unzeta, E. Gálvez, J. Marco-Contelles, *Eur. J. Med. Chem.* **2011**, *46*, 4665.
- [20] J. Sterling, Y. Herzig, T. Goren, N. Finkelstein, D. Lerner, W. Goldenberg, I. Miskolczi, S. Molnar, F. Rantal, T. Tamas, G. Toth, *J. Med. Chem.* **2002**, *45*, 5260.
- [21] L. Emilsson, P. Saetre, J. Balciuniene, A. Castensson, N. Cairns, E. E. Jazin, *Neurosci. Lett.* **2002**, *326*, 56.
- [22] E. Borroni, B. Bohrmann, F. Grueninger, E. Prinssen, S. Nave, H. Loetscher, S. J. Chinta, S. Rajagopalan, A. Rane, A. Siddiqui, B. Ellenbroek, *J. Pharmacol. Exp. Ther.* **2017**, *362*, 413.

- [23] M. S. Uddin, M. T. Kabir, M. M. Rahman, B. Mathew, M. A. Shah, G. M. Ashraf, *J. Pharm. Pharmacol.* **2020**, *72*, 1001.
- [24] M. S. Manhas, S. N. Ganguly, S. Mukherjee, A. K. Jain, A. K. Bose, *Tetrahedron Lett.* **2006**, *47*, 2423.
- [25] H. O. Gulcan, S. Unlu, E. Banoglu, M. F. Sahin, E. Kupeli, E. Yesilada, *Turk. J. Chem.* **2003**, *27*, 467.
- [26] H. O. Gulcan, E. Kupeli, S. Unlu, E. Yesilada, M. F. Sahin, *Arch. Pharm.* **2003**, *336*, 477.
- [27] S. Carradori, M. D'Ascenzio, P. Chimenti, D. Secci, A. Bolasco, *Mol. Divers.* **2014**, *18*, 219.
- [28] I. Bolea, A. Gella, M. Unzeta, *J. Neural Transm.* **2013**, *120*, 893.
- [29] S. Zhou, G. Chen, G. Huang, *Bioorg. Med. Chem.* **2018**, *26*, 4863.
- [30] D. D. Soto-Ortega, B. P. Murphy, F. J. Gonzalez-Velasquez, K. A. Wilson, F. Xie, Q. Wang, M. A. Moss, *Bioorg. Med. Chem.* **2011**, *19*, 2596.
- [31] R. F. Guíñez, M. J. Matos, S. Vazquez-Rodriguez, L. Santana, E. Uriarte, C. Olea-Azar, J. D. Maya, *Future Med. Chem.* **2011**, *5*, 1911.
- [32] F. Orsini, L. Verotta, K. Klimo, C. Gerhäuser, *Arch. Pharm.* **2016**, *349*, 414.
- [33] Schrödinger Release 2018-1, Schrödinger, LLC, New York, NY **2018**.
- [34] O. Gerlits, K.-Y. Ho, X. Cheng, D. Blumenthal, P. Taylor, A. Kovalevsky, Z. Radić, *Chem.-Biol. Interact.* **2019**, *309*, 108698. <https://doi.org/10.1016/j.cbi.2019.06.011>
- [35] D. Knez, N. Coquelle, A. Pišlar, S. Žakelj, M. Jukič, M. Sova, J. Mravljak, F. Nachon, X. Brazzolotto, J. Kos, J.-P. Colletier, S. Gobec, *Eur. J. Med. Chem.* **2018**, *156*, 598. <https://doi.org/10.1016/j.ejmech.2018.07.033>
- [36] J. Reis, F. Cagide, J. Mialet-Perez, E. Uriarte, A. Parini, F. Borges, C. Binda, *J. Med. Chem.* **2018**, *61*, 4203. <https://doi.org/10.1021/acs.jmedchem.8b00357>
- [37] H. M. Berman, J. Westbrook, Z. Feng, G. Gilliland, T. N. Bhat, H. Weissig, I. N. Shindyalov, P. E. Bourne, *Nucleic Acids Res.* **2000**, *28*, 235.
- [38] Schrödinger Release 2018-1: Protein Preparation Wizard; Epik, Schrödinger, LLC, New York, NY **2016**; Impact, Schrödinger, LLC, New York, NY **2016**; Prime, Schrödinger, LLC, New York, NY **2018**.
- [39] Schrödinger Release 2018-1: LigPrep, Schrödinger, LLC, New York, NY **2018**.
- [40] Schrödinger Release 2018-1: ConfGen, Schrödinger, LLC, New York, NY **2018**.
- [41] K. S. Watts, P. Dalal, R. B. Murphy, W. Sherman, R. A. Friesner, J. C. Shelley, *J. Chem. Inf. Model.* **2010**, *50*, 534.
- [42] Schrödinger Release 2018-1: Glide, Schrödinger, LLC, New York, NY **2018**.
- [43] Schrödinger Release 2018-1: Prime, Schrödinger, LLC, New York, NY **2018**.

### SUPPORTING INFORMATION

Additional supporting information may be found online in the supporting information tab for this article.

**How to cite this article:** Shukur KT, Ercetin T, Luise C, et al. Design, synthesis, and biological evaluation of new urolithin amides as multitarget agents against Alzheimer's disease. *Arch Pharm.* 2021;354:e2000467. <https://doi.org/10.1002/ardp.202000467>